Available online at www.sciencedirect.com

ScienceDirect

Energy Procedia 142 (2017) 1474–1481

Energy Procedia

www.elsevier.com/locate/procedia

9th International Conference on Applied Energy, ICAE2017, 21-24 August 2017, Cardiff, UK

Numerical investigation of a looped-tube traveling-wave thermoacoustic generator with a bypass pipe

Ali Al-Kayiem, and Zhibin Yu*

School of Engineering, University of Glasgow, Glasgow, Scotland, United Kingdom

Abstract

In this paper, based on the recent development of looped-tube thermoacoustic engine with a bypass pipe, we propose and numerically demonstrate a travelling wave thermoacoustic electric generator using this configuration. It essentially employs a one wave-length travelling-wave acoustic resonator which has low acoustic losses. The engine branch consists of a compliance, a inertance tube, an engine core, and an alternator. An ultra-compliant alternator (i.e., a sub-woofer) is installed in the acoustic compliance section where the local acoustic impedance is relatively low but the cross sectional area is big. The numerical simulations demonstrate its working principle, and show that it can potentially achieve comparable performance as other types of travelling wave thermoacoustic electric generators.

Peer-review under responsibility of the scientific committee of the 9th International Conference on Applied Energy.

Keywords: *Travelling-wave, thermoacoustic engine, alternator, generator*

1. Introduction

Travelling wave thermoacoustic engine is essentially an acoustic equivalent of the conventional Stirling engine. It uses a compact acoustic network to modulate a sound wave and force to propagate through a regenerator with a steep temperature gradient imposed a pair of hot and ambient heat exchangers. The complicated interactions between the acoustic and temperature fields force the gas parcels to experience a Stirling like thermodynamic cycle at microscopic level, converting thermal energy to acoustic power (i.e., a form of p-v power) at macro scale level. The generated

* Corresponding author. Tel.: +44-0-141 330 2530.
E-mail address: Zhibin.Yu@glasgow.ac.uk

Peer-review under responsibility of the scientific committee of the 9th International Conference on Applied Energy.
10.1016/j.egypro.2017.12.595

acoustic power can be utilized to either drive thermoacoustic heat pump to upgrade heat from low to high temperature, or drive a transducer to produce electricity.

Various geometrical configurations have been proposed for developing travelling wave thermoacoustic engines, such as looped-tube traveling wave engine [1], multi-stage lopped-tube engines [2], Backhaus and Swift's torus type engine [3], looped-tube engine with a bypass pipe [4, 5], etc. Several different types of transducers have also been proposed to develop travelling wave thermoacoustic electric generators, including high impedance linear alternators [6], ultra-compliant audio loudspeakers [7, 8], and piezoelectric generators [9], etc. The integration of different engine configurations with different transducers have led to the development of a number of different travelling wave electric generators, and it remains a hot research topic.

In this paper, we propose to integrate a looped-tube travelling wave engine having a bypass pipe [4, 5] with an ultra-compliant transducer (i.e., a sub-woofer) to develop a new type of traveling wave thermoacoustic electric generator. The concept is firstly described and explained, and then a prototype is modelled and designed using DeltaEC software (Design Environment for Low-amplitude ThermoAcoustic Energy Conversion) [10]. Its working principle is demonstrated and its performance is then analyzed numerically.

2. Concept

As shown in Fig.1, this looped-tube engine has a hot heat exchange (HHX), a regenerator (REG), an ambient heat exchanger (AHX), a thermal buffer tube (TBT), and secondary ambient heat exchanger (2nd AHX). The system also has a feedback pipe, a bypass pipe, a compliance volume, and an inertance tube. The arrows indicate the acoustic power flow. In this paper, a low-impedance transducer (i.e., sub-woofer) [7, 8] is coupled to the engine to develop an electric generator. The compliance volume has relatively low acoustic impedance and a larger cross sectional area, which is ideal for installing such a low impedance alternator. As such, the alternator housing can also work as a compliance volume.

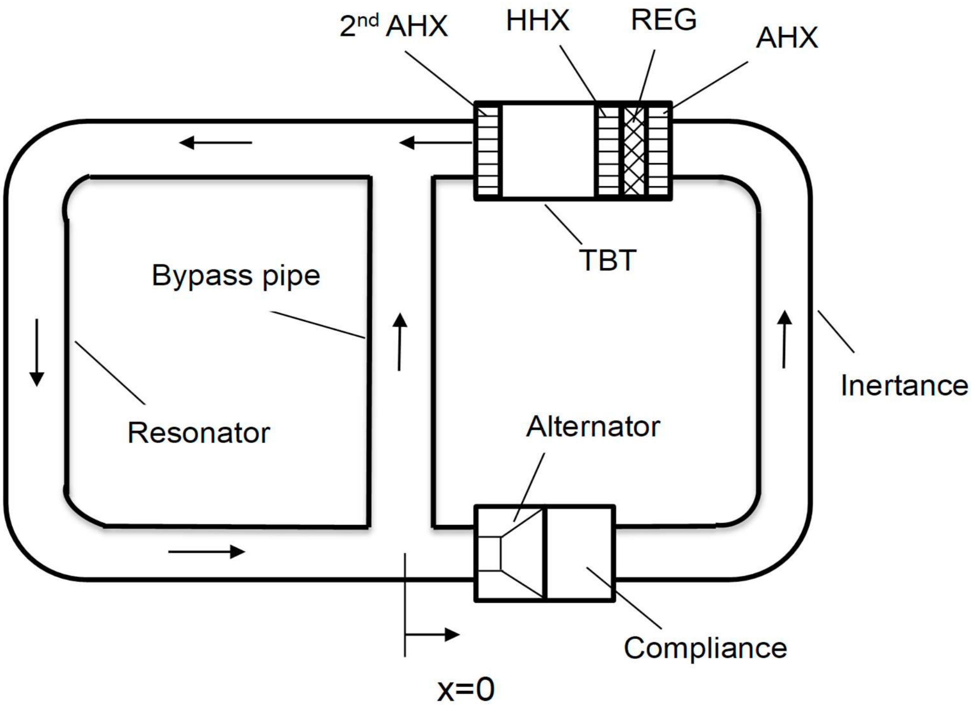

Fig.1. Schematic diagram of a looped-tube thermoacoustic electric generator with a by-pass pipe.

A prototype has been modelled in this paper. The dimensions of its main components are summarised in Table 1. The parameters of the alternator are listed in Table 2, which are properties based on an actual subwoofer (B&C 8NW51 [11]) with slight changes to match acoustic characteristics of the engine. The parameters are believed to be achievable using audio loudspeaker manufacture technologies as subwoofers with similar parameters are widely available in the market [7].

The heat source temperature (i.e. the solid temperature at HHX) is set as about 624 ℃, and heat sink temperature (i.e., the solid temperature of AHX and 2nd AHX) is set as 28 ℃. The working gas is nitrogen at a pressure of 10 bar, and the operating frequency is set as 76.5 Hz. The heat input to the hot heat exchanger is set as around 1100 W.

Table1. The dimensions of the system's components.

Part	Diameter (m)	Length (mm)	r_h (um)	Porosity
REG	0.138	19.7	30	0.77
AHX	0.138	21	700	0.5
HHX	0.138	20	800	0.5
SAHX	0.138	21	700	0.5
Part	Diameter (mm)		Length (cm)	
Bypass	55.2		100	
Resonator	71.3		244	
Inertance	40.68		165	
Compliance	107		28	
TBT	138		5	

Table 2: Parameters of the linear alternator used in the research [11] B&C Speakers.

Parameter	Symbol	Unit	Value
Resonance frequency	F_s	Hz	74
Force factor	Bl	N/A	30
Electric inductance	L_e	mH	0.6
Electric resistance	R_e	Ω	4.2
Moving mass	M_m	g	30
Stiffness	k_m	mm/N	7500
Mechanical resistance	R_m	kg/s	0.8
Maximum excursion	X_{max}	mm	5.7
Effective area	S	cm^2	150

3. Simulation results

After a series of optimization steps which are omitted here, the final simulation results of an optimized model are summarized in Table 3. The engine receives around 1100 W of heating power, and generates 166 W electricity. Some typical simulation results are presented in this section to demonstrate the working principle of the system, as shown in Figure 2.

Figure 2 (a) demonstrates the acoustic power flow along the loop. About 465 W of acoustic power enters the alternator housing and it dissipates around 13 W. The alternator extracts about 237 W of acoustic power and produces 166 W of electricity with an acoustic-to-electricity efficiency η_{a-e}=70%. (Although this power level is too large for a sub-woofer without any modification, the results are interesting given that such ultra-compliant linear alternator can be built in the future [7].) The remaining 227 W acoustic power feeds into the cold heat exchanger and it dissipates about 6 W. About 210 W acoustic power flows into the regenerator where it is amplified to around 514W. On the other hand, about 75.7 W of the acoustic power is shunted to the bypass. After some dissipation in it, about 60 W acoustic power exits it and joins with the acoustic power comes out from the secondary ambient heat exchanger. Finally, around 556 W of acoustic power goes to the feedback pipe. The net acoustic power production from the engine unit is about 288 W. This ultimately leads to the engine efficiency is 21.5%, which is about 32.4% of the Carnot efficiency for these heat sources and sink temperatures. As a result, the thermal-to-electricity efficiency η_{h-e}=15%.

(a)
(b)
(c)
(d)
(e)

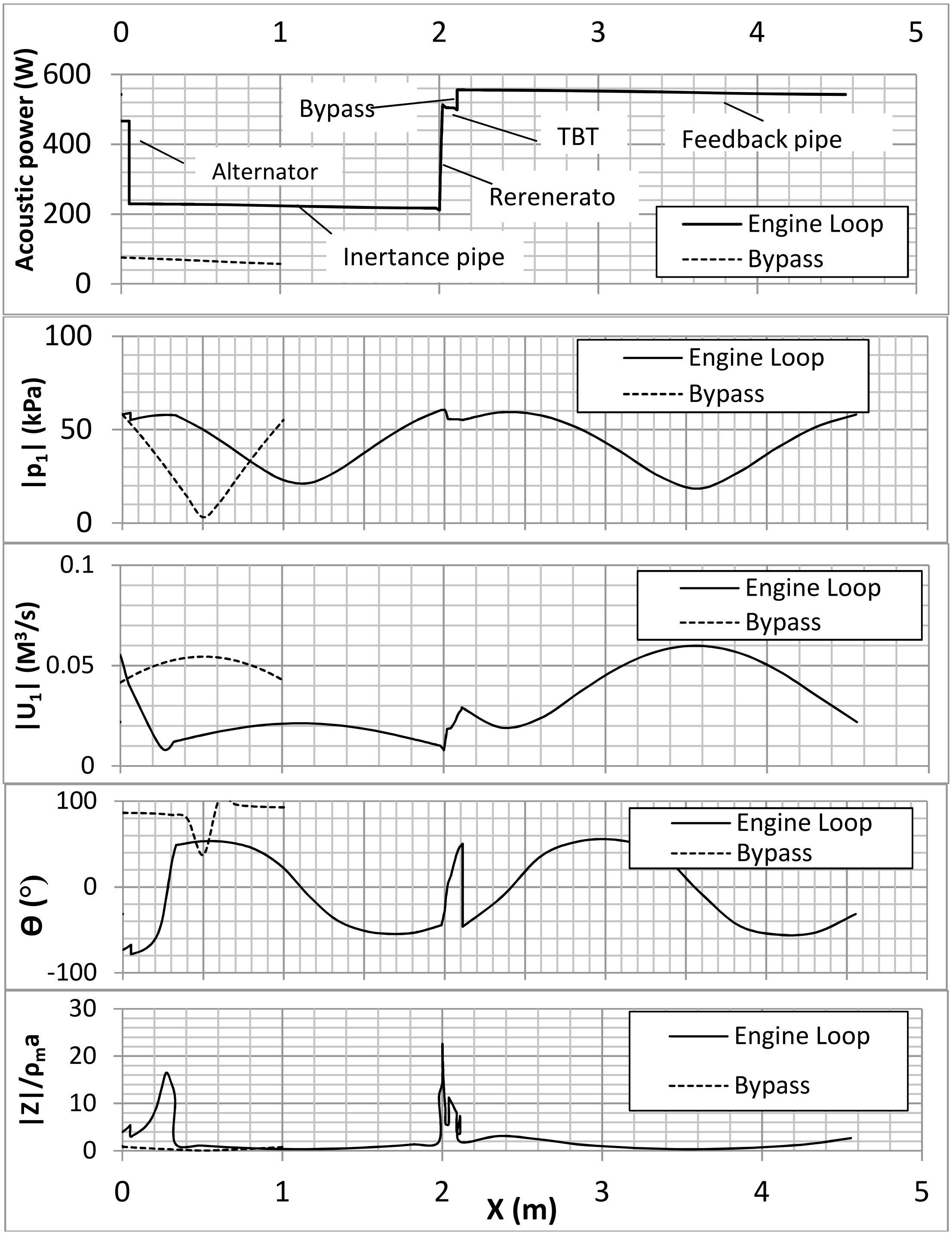

Fig.2. Simulation results of the acoustic field: (a) acoustic power flow, (b) pressure amplitude, (c) volumetric velocity, (d) phase angle between pressure and velocity, and (e) normalised acoustic impedance.

Figure 2 (b) presents the acoustic pressure distribution along the system. The maximum value of pressure is 61 kPa at the engine core, and the minimum value is 3 kPa at the middle of the by-pass pipe, resulting pressure amplitude ratio around 2.3. In a ideal travelling wave field, this ratio should be 1. This means that the acoustic reflection within the resonator is still relatively high.

Figure 2 (c) shows the distribution of the amplitude of volumetric velocity along the system. It can be seen that the by-pass pipe shunts only one seventh of the volumetric velocity at the end of the feedback pipe (X=0). As a result, a small part of the acoustic power (i.e., 75.7 W) flows to the bypass and the rest (i.e., 466.8 W) acoustic flows into the engine branch.

Figure 2 (d) shows the phase difference between the pressure and velocity oscillations along the system. It can be noticed that phase angle is in the range $-55° < \Theta < 55°$ along the feedback pipe, and $-45° < \Theta < 50°$ within the engine branch. It can be found that the phase angles in this thermoacoustic generator system is a bit far away from the ideal travelling wave conditions, which indicates that the alternator has strongly altered the acoustic field along the system. This can be attributed to the fact that the alternator causes a large pressure drop but has the same volumetric velocity at its two sides [7], and thus strong acoustic reflections are induced. Further investigation is required to understand how the altered acoustic field can be corrected in the future. For example, a side-branched stub may be added to cancel the alteration introduced by the alternator [7].

Figure 2 (e) shows the normalised acoustic impedance along the system. There are two high acoustic impedance regions along the system. One is around the engine core with $\rho_{\mathrm{ma}} = 23$, and the other is within the alternator housing with $\rho_{\mathrm{ma}} = 16$, which is in line with the results shown in Figure 2 (c-e). It can also be seen that the alternator causes a sharp drop of the acoustic impedance as expected. As proposed by Backhaus, to reduce the acoustic losses with in the regenerator, the acoustic impedance should be in the range of 15-30 times of $\rho_{\mathrm{m}}a$ within the regenerator [3].

Table 3: Summary of simulation results of the thermoacoustic electric generator.

Symbol	Definition	Unit	Engine	Alternator
T_h	Solid Temperature at HHX	°C	624	N/A
T_a	Solid Temperature at AHX	°C	28	N/A
$W_{a,\,in}$	Acoustic power inlet	W	217	467
$W_{a,\,out}$	Acoustic power outlet	W	505	230
$W_{a,\,net}$	Net acoustic power production (engine) or consumption (alternator)	W	288	237
W_e	Electrical power production	W	N/A	166
$Q_{in,i}$	Heat input to HHX (engine)	W	1100.7	N/A
η_e	Engine Efficiency	%	21.5	
$\eta_{a\text{-}e}$	Alternator efficiency	%	70	
η_{Carnot}	Carnot Efficiency: $(T_{\mathrm{h}}-T_{\mathrm{a}})/T_{\mathrm{h}}$	%	66.4	
η_r	Percentage of Carnot Efficiency	%	32.4	

4. Effects of several key parameters

To further demonstrate the design of this system, a few typical optimization steps are presented here. The lengths of the bypass pipe, inertance tube, the compliance, and the thermal buffer tube, as well as the operating frequency have been optimized when the electric power generation from the generator is used as a performance indictor. For each round of optimization, one parameter is swept in a range when the rest of the parameters are kept constant. The obtained results are shown in Figures 3-5.

Figure 3 (a) shows the effect of the length of the bypass pipe on the electric power output. The optimal length is about 1 m and it is selected for final design. It can be noticed that the generated electric power increases dramatically till it reaches a maximum value 126 W when the optimal by-pass length is 1 m, and it then decreases gradually when the by-pass length increases further.

Similarly, Figure 3 (b) shows the relationship between length of the inertance tube and electric power output. The results lead to an optimal length about 1.65 m. The bypass and inertance tube are the components affecting the phase angle between the pressure and velocity oscillations. Their dimensions are very sensitive for achieving the right phase and impedance within the engine and the feedback pipe.

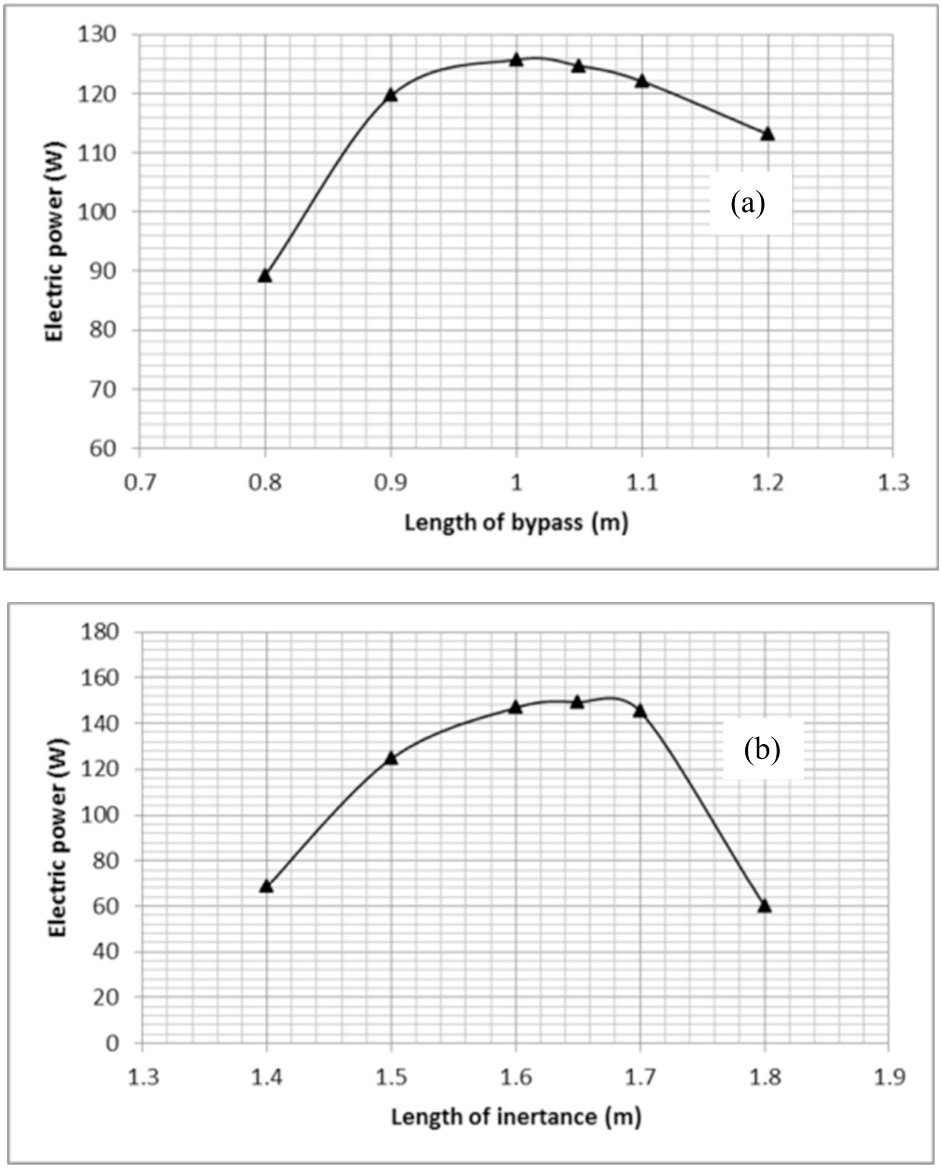

Fig.3. Electric power output as function of (a) the length of the bypass pipe and (b) length of the inertance tube.

Figure 4 (a) shows the relationship between length of the compliance and electric power output. The optimal length is about 0.281 m and it is selected for final design. In the same way, Figure 4 (b) shows the relationship between length of the thermal buffer tube and electric power output. The results lead to an optimal length about 0.05 m and it was selected for the final design.

Figure 5 shows the relationship between the electric power output and the operating frequency of the system. The feedback pipe length has been varied to change the operating frequency of the system. It can be seen from Figure 5 that the electric power output firstly increases with the frequency rapidly. It reaches a maximum value 162 Watts when the optimal frequency is about 76.5 Hz, and it then decreases sharply when frequency increases further. Referring to Table 2, one can find that the optimal operating frequency is very close to the resonance frequency of the alternator.

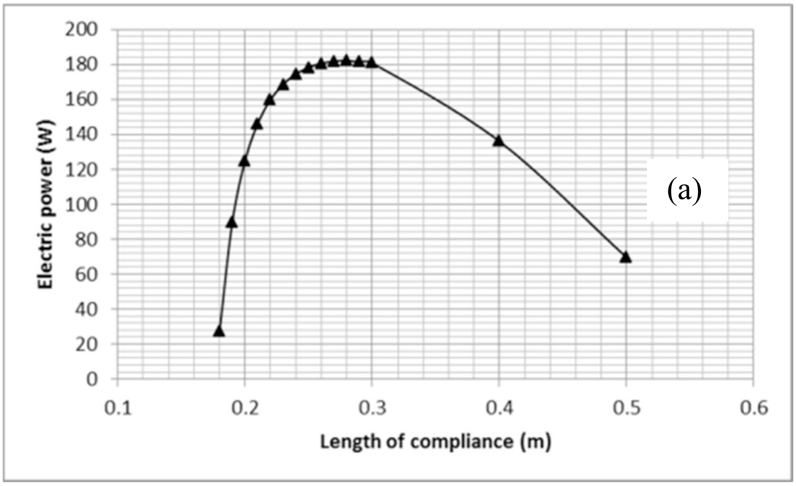

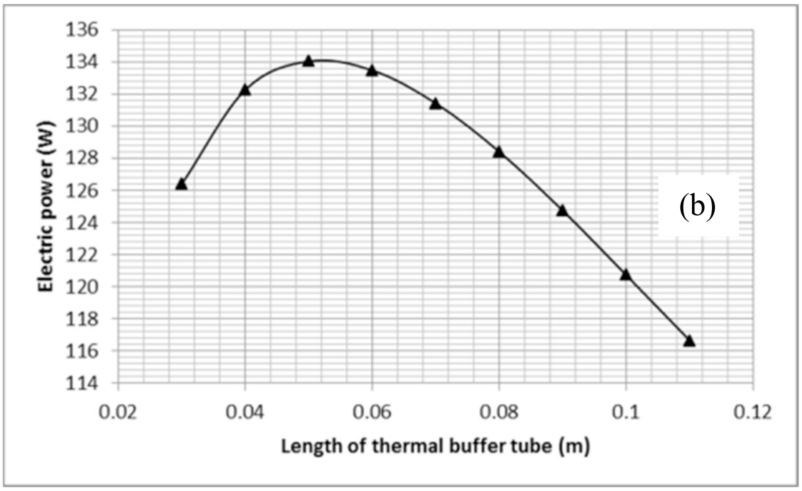

Fig.4. Electric power output as function of the (a) length of the compliance; (b) length of the thermal buffer tube.

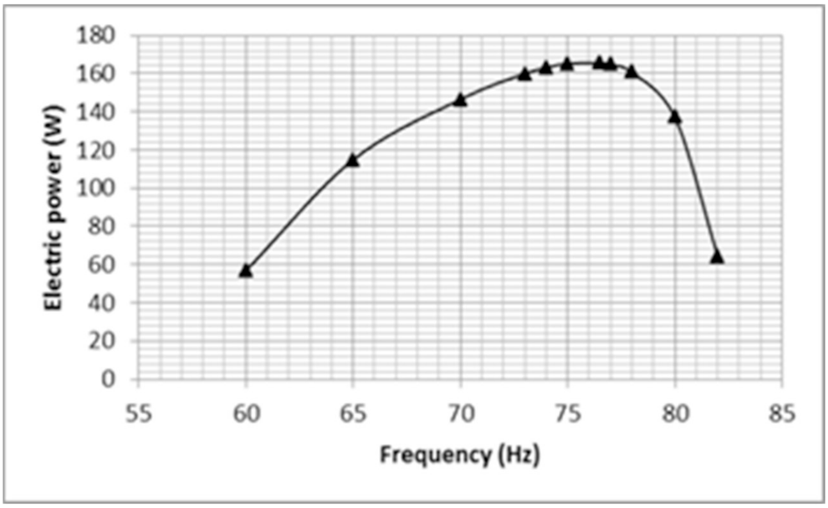

Fig.5. Electric power output as function of the operating frequency.

5. Conclusions

This paper presents a comprehensive numerical analysis of a looped-tube travelling wave thermoacoustic generator with a bypass pipe. The numerical simulations show that the system can achieve a thermal efficiency of 21.5% when the heat is added to the system at 624 °C, which is equivalent to 32.4% of the Carnot efficiency under the same operating conditions. The alternator extracts 237 W acoustic power from the engine and generates 166 W electricity, which ultimately leads to an alternator efficiency of about 70%. The overall thermal-to-electric efficiency was about 15%, which are comparable to the experimental results of other types of travelling wave thermoacoustic generators. The present research demonstrated that travelling wave thermoacoustic engine with such a configuration can achieve comparable performances as other types of travelling wave thermoacoustic engines. The future work will be focused on constructing a prototype to experimentally demonstrate the system as designed in this paper.

Acknowledgements

Ali Al-Kayiem would like to acknowledge the finance support from the Ministry of Higher of Education/Babylon University in Iraq (Reference: 553, Iraqi cultural attaché).

References

[1] Yazaki T, Iwata A, Maekawa T, Tominaga A. Traveling wave thermoacoustic engin in a looped tube. Phys Rev Lett 1998; 81:3128–31.
[2] De Blok K. Novel 4-stage traveling wave thermoacoustic power generator. In: Proceedings of ASME 2010 3rd joint US-European fluids engineering summer meeting and 8th international conference on nanochannels, microchannels and minichannels, FEDSM2010-ICNMM2010, Montreal, Canada; August 2–4, 2010.
[3] Backhaus S, Swift GW. A thermoacoustic-Stirling heat engine: detailed study.J Acoust Soc Am 2000;107:3148-3166.
[4] De Blok K. Low operating temperature integral thermoacoustic devices for solar cooling and waste heat recovery. J Acoust Soc Am 2008;123(5):3541.
[5] Al-Kayiem A, Yu Z, Numerical investigation of a looped-tube travelling-wave thermoacoustic engine with a bypass pipe Energy 112, 111-120
[6] Backhaus S, Tward E, Petach M. Travelling-wave thermoacoustic electricgenerator. Appl Phys Lett 2004;85(6):1085–7.
[7] Yu Z, Jaworski AJ, Backhaus S. Travelling-wave thermoacoustic electricity generator using an ultra-compliant alternator for utilization of low-grade thermal energy. Applied Energy 2012; 99:135-145.
[8] Kang H, Cheng P, Yu Z, Zheng H. A two-stage traveling-wave thermoacoustic electric generator with loudspeakers as alternators. Appl Energy 2015;137: 9-17.
[9] Jensen C, Raspet R. Thermoacoustic power conversion using a piezoelectric transducer. J Acoust Soc Am 2010;128:98–103.
[10] Ward B, Clark J, Swift G. Design environment for low-amplitude thermoacoustic energy conversion, DELTAEC version 6.2: users guide. Los Alamos National Laboratory; 2008.
[11] B&C Speakers. http://www.bcspeakers.com.